GDCh

Communications

Angewandte
Chemie
International Edition
www.angewandte.org

Tautomerism | Hot Paper

Shape-Shifting Molecules: Unveiling the Valence Tautomerism Phenomena in Bare Barbaralones

Miguel Sanz-Novo, Mauro Mato, Íker León, Antonio M. Echavarren, and José L. Alonso*

Abstract: We report a state-of-the-art spectroscopic study of an archetypical barbaralone, conclusively revealing the valence tautomerism phenomena for this bistable molecular system. The two distinct 1- and 5-substituted valence tautomers have been isolated in a supersonic expansion for the first time and successfully characterized by high-resolution rotational spectroscopy. This work provides irrefutable experimental evidence of the [3,3]-rearrangement in barbaralones and highlights the use of rotational spectroscopy to analyze shape-shifting mixtures. Moreover, this observation opens the window toward the characterization of new fluxional systems in the isolation conditions of the gas phase and should serve as a reference point in the general understanding of valence tautomerism.

Dynamic covalent chemistry (DCvC) is a coveted synthetic strategy that has attracted many theoretical and experimental studies for around a century.[1] It plays a key role in developing intricate supramolecular assemblies from discrete molecular building blocks.[2] Among all DCvC processes, we targeted the valence tautomerism. This phenomenon, which lies under the umbrella of sigmatropic rearrangements, consists of an intramolecular rearrangement, giving rise to an usually different molecular structure (see Figure 1).

In this context, barbaralone, bullvalone, and bullvalene, widely well-known fluxional or "shape-shifting" molecules,

[*] M. Sanz-Novo, Dr. Í. León, Prof. J. L. Alonso
Grupo de Espectroscopía Molecular (GEM), Edificio Quifima, Área de Química-Física, Laboratorios de Espectroscopía y Bioespectroscopía, Parque Científico UVa, Unidad Asociada CSIC, Universidad de Valladolid, 47011, Valladolid (Spain)
E-mail: jlalonso@qf.uva.es

Dr. M. Mato, Prof. A. M. Echavarren
Institute of Chemical Research of Catalonia (ICIQ),
Barcelona Institute of Science and Technology,
Av. Països Catalans 16, 43007 Tarragona (Spain)
and
Departament de Química Analítica i Química Orgànica,
Universitat Rovira i Virgili, C/Marcel·li Domingo s/n,
43007 Tarragona (Spain)

have been deeply ingrained in understanding the valence tautomerism phenomena.[3,4] These structurally unique dynamic molecules can interconvert among different constitutional isomers through low-energy strain-assisted Cope rearrangements ([3,3]-sigmatropic rearrangements). For instance, 1.2 million degenerate isomers are anticipated for bullvalene.[3d] However, a lower number of valence tautomers exist for substituted bullvalenes,[5–7] and only two discrete species are expected for barbaralone.[8] So far, valence-tautomerism phenomena have been investigated in the condensed phases by NMR and X-ray diffraction experiments.[9–12] It is well known that modern NMR spectroscopy has become the chemist's "choice by default" when it comes to the description of a chemical structure as well as the dynamics of molecular systems. The successful determination of dynamic parameters depends on whether the target process is faster or slower than the corresponding NMR time scale. For fast processes, a simplified NMR spectrum is observed, which typically de-coalesce into a more complex, and therefore informative, array of peaks when the temperature of the experiment is decreased.[5] Nevertheless, the dynamic equilibria may be perturbed due to interactions with the environment.

The prior scenario highlights the need of a benchmark investigation on a fluxional system to decipher its intrinsic structural properties, therefore precluding laborious spectroscopic interpretations. Thus, to understand the structure of these molecular architectures, it is desirable first to study these systems in the absence of intermolecular interactions. Gas-phase experiments will enable the study of each structure involved in the dynamic equilibria separately instead of trying to deconvolute those equilibria in the condensed phase. They should represent an essential source of reference data to unveil the phenomena of valence
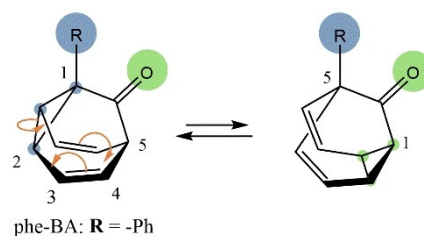

phe-BA: **R** = -Ph

Figure 1. Valence tautomerism of 1-substituted barbaralones, showing the redistribution of bonding electrons ascribed to the sigmatropic equilibrium. As shown, a σ-bond migrates, leading to a reorganization of the two π-bonds, but the sequence of atoms within the carbon cage remains unchanged.

tautomerism, especially those involving very fast rearrangements under normal conditions.

In the present work, we report the first experimental investigation of the archetypal phenyl-substituted barbaralone (phe-BA from now) isolated in the gas phase to shed light on these shape-shifting molecular systems. Rotational spectroscopy has proven a powerful tool for unambiguously identifying chemical species in the gas phase and is acknowledged among the most robust techniques to distinguish between subtle changes in molecular geometry. Since every molecule has a unique three-dimensional structure, it possesses a characteristic set of rotational constants. The major problem of working with gas-phase barbaralones is the labile nature of their solid samples and inherent vaporization difficulties. Fourier-transform microwave spectroscopy, coupled with laser-ablation techniques, breaks through the limitation of placing nonvolatile molecules in the gas phase, unraveling the most stable conformers generated in a supersonic expansion.[13,14] To date, detailed structural and conformational information has been reported on many building blocks using this experimental approach.[15–19] The beauty of this approach is that the spectral assignments rely on the consistency of hundreds of observed rotational lines. In our particular case of study, different constitutional isomers, if they are enough populated in the supersonic expansion, will present distinct spectroscopic constants and can be therefore unequivocally identified without any spectral overlap. The usefulness of rotational spectroscopy is that it allows discerning between similar molecules with minimal structural changes. This fact is strongly supported by the experimental observation of the tautomeric properties of several nitrogen bases and creatinine.[20a,b] Even very similar compounds such as the 1- and 5-valence tautomers of the phe-BA (see Figure 1) should be readily distinguished on this basis.

Phe-BA was synthesized following our previously reported strategy[21] to generate substituted barbaralones by a gold(I)-catalyzed oxidative cyclization of 7-alkynyl-1,3,5-cycloheptatrienes, which are powerful precursors of barbaralyl-cation intermediates.[22] We employed our laser ablation chirped-pulse Fourier transform microwave (LA-CP-FTMW) spectrometer[23] to record the broadband spectrum from 2.0 to 7.0 GHz of the solid phe-BA (m.p. 108–110 °C), shown in Figure 2. Besides several intense ^cR-branch line progressions, it was straightforward to identify strong ^cQ-branch progressions (see Figure 2) ascribable to a first rotameric species labeled as **I**. Also, characteristic progressions of ^aR-branch transitions ranging from $J'' = 1$ to $J'' = 7$ were quickly recognized and attributed to the same rotamer. Up to 147 rotational transitions were collected, and subsequently, least-squares fitted to semirigid-rotor Hamiltonian.[24] The determined spectroscopic constants are listed in the first column of Table 1.

The values of the rotational constants of rotamer **I** are consistent with those expected for a sizeable molecular species such as phe-BA. Nevertheless, the two candidate structures exhibit minimal structural differences in the carbon cages (see Figure 1) that should induce a small but specific change in the values of the rotational constants, significant enough to allow conclusive discrimination. Within this framework and concurrent to the experimental work, theoretical calculations were carried out on the two plausible 1- and 5- substituted phe-BA tautomers. We explored the potential energy surface (PES) of each tautomer separately using fast molecular-mechanics methods. For both systems, only one single conformation was found below an energetic window of 1000 cm^{-1}. Then, we executed geometry optimizations for the 1- and 5-phe-BA tautomers using high-level theoretical computations, performed using Gaussian 16 (Revision A.03) program package[25] (see

Table 1: Experimental spectroscopic parameters of the phe-BA tautomers compared with those theoretically predicted for the lowest-in-energy structures.

Parameters	Experimental		Theory[g]	
	Rotamer **I**	Rotamer **II**	**1-phe-BA**	**5-phe-BA**
$A^{[a]}$/MHz	1274.35677 (46)[f]	1331.6505 (10)	1271.7	1327.5
B/MHz	388.10352 (12)	394.31620 (45)	387.5	392.3
C/MHz	379.62560 (12)	381.92829 (41)	378.5	380.8
Δ_{JK}/kHz	0.0742 (22)	–	–	–
Δ_K/kHz	−5.519 (28)	–	–	–
$|\mu_a|$/D	observed	not observed	1.2	2.5
$|\mu_b|$/D	not observed	not observed	0.0	0.0
$|\mu_c|$/D	observed	observed	3.1	2.6
$P_c^{[b]}$	183.747	168.971	183.2	170.9
$\sigma^{[c]}$/kHz	10.7	14.4	–	–
$N^{[d]}$	147	43	–	–
$\Delta E^{[e]}$/kcal mol^{-1}	–	–	0.0	2.6

[a] A, B, and C represent the rotational constants (in MHz); μ_a, μ_b, and μ_c are the electric dipole moment components (in D). [b] P_c is the planar inertial moment (in u Å^2) with respect to the ab symmetry plane, computed using the following equation: $P_c = \frac{1}{2}\,(I_a + I_b - I_c)$. Conversion factor: 505 379.1 MHz u Å^2. [c] RMS deviation of the fit (in kHz) using a Hamiltonian in the Watson's A-reduction, I^r-Representation. [d] Number of measured transitions. [e] Relative energies (in kcal mol^{-1}) concerning the global minimum, taking into account the zero-point energy (ZPE). [f] Standard error in parentheses in units of the last digit. [g] Theoretical computations were conducted at the B3LYP-GD3/aug-cc-pVTZ level of theory.
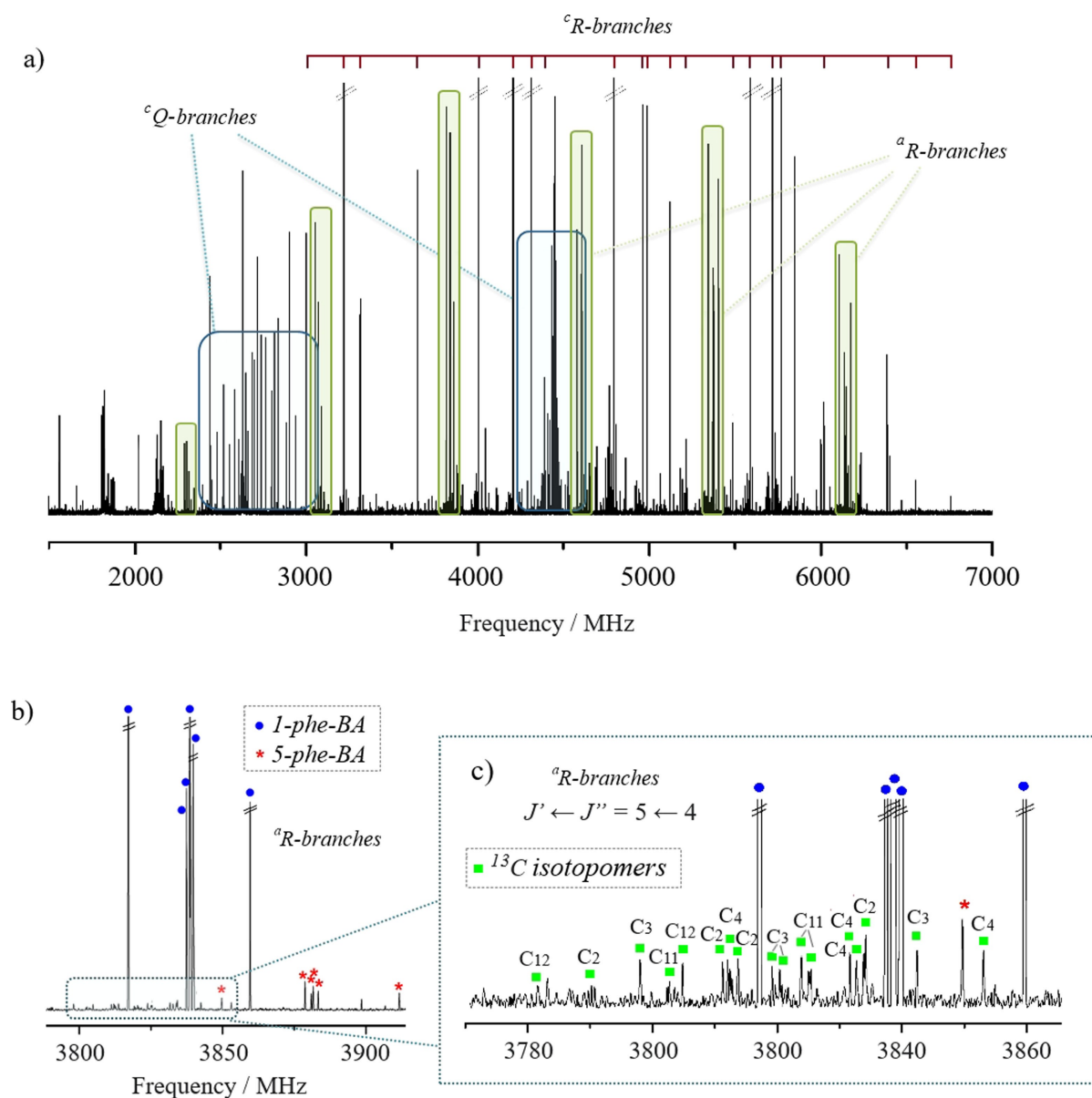
Figure 2. a) Jet-cooled broadband LA-CP-FTMW rotational spectrum of BA from 1.5 to 7.0 GHz, where intense ^{c}Q-branches are remarked in blue, ^{a}R-branch progressions are highlighted in green and intense ^{c}R-branch lines are indicated in garnet. b) Section of the broadband spectrum showing a comparison of strong ^{a}R-branch transitions ($J'\leftarrow J''=5\leftarrow4$) for both tautomers, 1-phe-BA (in blue) and 5-phe-BA (in red). c) Zoomed view showing the same ^{a}R-branch transitions of the ^{13}C isotopomers of 1-phe-BA (in green). The intensity is in arbitrary units.

Supporting Information for detailed information). The predicted spectroscopic constants for 1- and 5-phe-BA are presented in Table 1 for comparison and the structures are depicted in Figure 3. We found an excellent matching between the experimental values of the rotational constants for rotamer **I** (first column of Table 1) and those theoretically predicted for 1-phe-BA. Scaling factors ranging from 1.001 to 1.003 bring the predicted DFT rotational constants values to the experimental ones, highlighting a remarkable resemblance which further supports the unequivocal identification.

At this point, an intriguing question arises: Is the 5-phe-BA tautomer present in the supersonic expansion? In a

quest to confirm the existence of the higher-in-energy tautomer, we removed the lines belonging to rotamer **I** and performed a thorough inspection in the low-intensity background of the spectrum. Strikingly, using the above scaling factors, much weaker rotational features attributable to a second rotamer **II** were found following a- and c-type dipole moment selection rules. Thus, we were able first to assign ^{a}R-branch $(J+1)_{0J+1}\leftarrow(J+1)_{0J}$ transitions, which are spaced approximately $B+C$ [see Figure 2b]. Subsequently, we extended the analysis to other a- and c-type lines and performed a least-square fit using a rigid-rotor approximation. We present the corresponding spectroscopic parameters in the second column of Table 1.
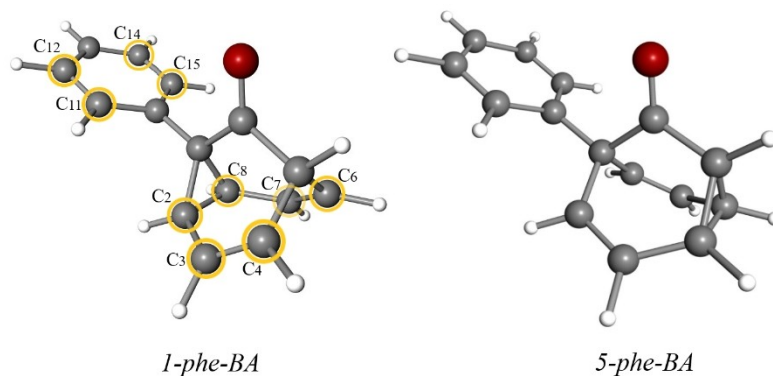
1-phe-BA   *5-phe-BA*

Figure 3. Structures of the two plausible valence tautomers: 1-substituted phe-barbaralone (1-phe-BA, left), 5-substituted phe-barbaralone (5-phe-BA, right). We named the different tautomers based on the position of the Ph substituent (see Figure 1). The equivalent carbons of 1-phe-BA (C_s symmetry) are marked with an orange circle.

In this case, the experimental rotational constants of rotamer **II** are in excellent agreement with those calculated for 5-phe-BA. Thus, following the abovementioned arguments, rotamer **II** can be directly ascribed to 5-phe-BA. Moreover, for rotamer **II**, *a*- and *c*-type lines showed relatively similar intensities, which is in good agreement with the resemblance of the μ_a and μ_c calculated dipole-moment components of 5-phe-BA (given in Table 1 for comparison). We have provided the first experimental evidence of the higher in energy tautomer based on a line-by-line assignment of over 40 discrete spectroscopic features. Finally, additional proof of the tautomeric identification comes from the P_c planar inertial moment values with respect to the *ab* symmetry plane. It varies from 183.74 to 168.97 $u\,Å^2$, in excellent agreement with the predicted values shown in Table 1. This remarkable theoretical-experimental synergy has been found in previous rotational studies[26a,b] and is in the context of a recent spectroscopic benchmark data base.[26c]

The relative abundances of both tautomers have been estimated by the relative intensity of a selected set of transitions.[20c,27] Therefore, we can estimate ratios of approximately 97:3 ± 1 between the 1- and 5-phenyl-barbaralone. Within this framework, this work offers definite experimental proof suggesting that the 1-substituted valence tautomer is the most stable tautomer, in accordance with the previous results reported by Ferrer and Echavarren.[21]

We finally discarded the lines belonging to 1- and 5-phe-BA and the weak intensity background of the broadband spectrum did not reveal the presence of other higher in energy predicted species (see Table S1 of the Supporting Information) nor plausible photofragmentation species.[28] However, on the low-frequency side of each ${}^aR$-branch line of 1-phe-BA [see Figure 1c for the $J'\leftarrow J''$ 5←4 transitions], we managed to identify very weak sets of transitions which could only be ascribed to the five pairs of ${}^{13}C$ isotopomers in their natural abundance (1.1%), showing doubled intensity due to their equivalent positions (C_s symmetry). The observed frequency shifts were consistent with those

predicted theoretically for 1-phe-BA. (see Table S2 of the Supporting Information). The cartesian coordinates of the substituted atoms are determined in the principal axis system using the Kraitchman equations[29] (see Table 2). The derived C–C bond lengths of the bonds implied in the electron migration are $d(C_2–C_3)=1.4805$ (21) Å and d-$(C_3–C_4)=1.3431$ (81) Å, which coincides with typical C–C and C=C bond lengths, respectively, further corroborating the identification of rotamer **I** as 1-phe-BA. The complete list of the measured experimental frequencies for both tautomers and the ${}^{13}C$ isotopomers are collected in Tables S3–S9 of the Supporting Information. A comparison between the gas-phase and solid-state geometric parameters (see Table S10 of the Supporting Information) shows a breakdown of the C_s symmetry in the crystal due to the lattice constraints.

In summary, we have provided compelling evidence of the shape-shifting rearrangement for an archetypal mono-substituted barbaralone through the use of rotational spectroscopy. Hence, the two distinct valence tautomers (1- and 5-substituted forms) have been unequivocally identified in the jet, showing that the most abundant species (1-phe-BA) matches the form expected along with the crystal structure. In addition, the C–C bond lengths involved in the π-bond reorganization have been precisely determined for the parent species, corroborating the identification of 1-phe-BA. Our investigation further suggests that substituted barbaralones are chemically robust yet structurally dynamic, which is an essential step toward their further use as starting materials and may bear implications in their chemical-physical properties in materials science. So far, NMR spectroscopy has been employed for the analysis of shape-shifting mixtures, but it is an arduous task to conclusively identify the individual structures rather than derive averaged chemical properties. However, as shown, the isolation conditions granted by the supersonic expansion enabled the study of each structure separately, instead of trying to deconvolute the dynamic equilibria in the condensed phase,[11,30] which may be perturbed due to interactions with

Table 2: Substitution structure of 1-phe-BA.

Atom	lal	lbl	lcl
C_2, C_8	0.9350 (17)[a]	0.7768 (21)	1.2714 (13)
C_3, C_7	2.16219 (79)	1.5260 (11)	0.9186 (19)
C_4, C_6	2.88180 (57)	1.2017 (14)	0.1681 (98)
C_{11}, C_{15}	1.9800 (12)	1.2050 (19)	0.105 (22)
C_{12}, C_{14}	3.37737 (70)	1.20190 (20)	0.107 (23)

Parameter	r_s	r_e[b]	
$r(C_2–C_3)$	1.4805 (21)	1.4713	
$r(C_3–C_4)$	1.3431 (81)	1.3344	
$r(C_{11}–C_{12})$	1.3974 (14)	1.3931	
$°(C_2–C_3–C_4)$	120.98 (15)	120.80	

[a] Standard error in parenthesis in units of the last digit. Bond distances are given in Angstroms (Å) and bond angles in degrees. [b] Equilibrium structure calculated at the B3LYP-GD3/aug-cc-pVTZ level. We show the equivalent carbon atoms due to the C_s symmetry of the molecule.

the environment. We are fiercely exploring the full scope and capabilities of rotational spectroscopy coupled to a laser-ablation vaporization source as a reliable characterization technique to unravel dynamic molecular systems. Further gas-phase studies exploring the valence-tautomerism equilibrium of relevant fluxional molecules will be undertaken to pave the route in the characterization of new shape-shifting species.

Conflict of Interest

The authors declare no conflict of interest.

Data Availability Statement

The data that support the findings of this study are available from the corresponding author upon reasonable request.

Keywords: Rotational Spectroscopy · Structure Elucidation · Tautomerism · Valence Isomerization

[1] a) S. J. Rowan, S. J. Cantril, G. R. L. Cousins, J. K. M. Sanders, J. F. Stoddart, *Angew. Chem. Int. Ed.* **2002**, *41*, 898–952; *Angew. Chem.* **2002**, *114*, 938–993; b) Y. Jin, C. Yu, R. J. Denman, W. Zhang, *Chem. Soc. Rev.* **2013**, *42*, 6634; c) K. Nikitin, R. O'Gara, *Chem. Eur. J.* **2019**, *25*, 4551–4589.

[2] Y. Jin, P. Taynton, W. Zhang, *Acc. Chem. Res.* **2014**, *47*, 1575–1586.

[3] a) W. von E. Doering, W. R. Roth, *Angew. Chem. Int. Ed. Engl.* **1963**, *2*, 115–122; *Angew. Chem.* **1963**, *75*, 27–46; b) R. V. Williams, *Chem. Rev.* **2001**, *101*, 1185–1204; c) D. A. Hrovat, E. C. Brown, R. V. Williams, H. Quast, W. T. Borden, *J. Org. Chem.* **2005**, *70*, 2627–2632; d) M. He, J. W. Bode, *Proc. Natl. Acad. Sci. USA* **2011**, *108*, 14752–14756.

[4] a) W. von E. Doering, W. R. Roth, *Tetrahedron* **1963**, *19*, 715–737; b) W. V. E. Doering, B. M. Ferrier, E. T. Fossel, J. H. Hatenstein, M. Jones Jr., G. Klumpp, R. M. Rubin, M. Saunders, *Tetrahedron* **1967**, *23*, 3943–3963.

[5] a) R. Poupko, H. Zimmermann, K. Mgller, Z. Luz, *J. Am. Chem. Soc.* **1996**, *118*, 7995–8005; b) K. Müller, H. Zimmermann, C. Krieger, R. Poupko, Z. Luz, *J. Am. Chem. Soc.* **1996**, *118*, 8006–8014; c) R. Poupko, K. Mgller, C. Krieger, H. Zimmermann, Z. Luz, *J. Am. Chem. Soc.* **1996**, *118*, 8015–8023; d) Z. Luz, L. Olivier, R. Poupko, K. Mgller, C. Krieger, H. Zimmermann, *J. Am. Chem. Soc.* **1998**, *120*, 5526–5538.

[6] a) B. Volkmann, G. Schrçder, *Chem. Ber.* **1984**, *117*, 2226–2232; b) K. Rebsamen, G. Schrçder, *Chem. Ber.* **1993**, *126*, 1419–1423; c) K. Rebsamen, G. Schrçder, *Chem. Ber.* **1993**, *126*, 1425–1427; d) K. Rebsamen, H. Rçttele, G. Schrçder, *Chem. Ber.* **1993**, *126*, 1429–1433.

[7] a) A. R. Lippert, J. Kaeobamrung, J. W. Bode, *J. Am. Chem. Soc.* **2006**, *128*, 14738–14739; b) A. R. Lippert, V. L. Keleshian, J. W. Bode, *Org. Biomol. Chem.* **2009**, *7*, 1529–1532; c) A. R. Lippert, A. Naganawa, V. L. Keleshian, J. W. Bode, *J. Am. Chem. Soc.* **2010**, *132*, 15790–15799; d) K. K. Larson, M. He, J. F. Teichert, A. Naganawa, J. W. Bode, *Chem. Sci.* **2012**, *3*, 1825–1828; e) M. He, J. W. Bode, *Org. Biomol. Chem.* **2013**, *11*, 1306–1317; f) J. F. Teichert, D. Mazunin, J. W. Bode, *J. Am. Chem. Soc.* **2013**, *135*, 11314–11321.

[8] a) J. B. Lambert, *Tetrahedron Lett.* **1963**, *4*, 1901–1906; b) J. C. Barborak, S. Chari, P. v R Schleyer, *J. Am. Chem. Soc.* **1971**, *93*, 5275–5277; c) H. Nakanishi, O. Yamamoto, *Chem. Lett.* **1975**, *4*, 513–516; d) C. Engdahl, P. Ahlberg, *J. Am. Chem. Soc.* **1979**, *101*, 3940–3946; e) E. R. Johnston, J. S. Barber, M. Jacomet, J. C. Barborak, *J. Am. Chem. Soc.* **1998**, *120*, 1489–1493.

[9] R. Poupko, H. E. Zimmermann, Z. Luz, *J. Am. Chem. Soc.* **1984**, *106*, 5391–5394.

[10] A. Müller, U. Haeberlen, H. Zimmerman, R. Poupko, Z. Luz, *Mol. Phys.* **1994**, *81*, 1239–1258.

[11] M. He, J. W. Bode, *Org. Biomol. Chem.* **2013**, *11*, 1306–1317.

[12] a) T. J. Katz, J. C. Carnahan, G. M. Clarke, N. Acton, *J. Am. Chem. Soc.* **1970**, *92*, 734–735; b) E. W. Turnblom, T. J. Katz, *J. Am. Chem. Soc.* **1973**, *95*, 4292–4311; c) S. A. Weissman, S. G. Baxter, A. M. Arif, A. H. Cowley, *J. Am. Chem. Soc.* **1986**, *108*, 529–531.

[13] a) J. P. Schermann, *Spectroscopy and Modelling of Biomolecular Building Blocks*, Elsevier, Amsterdam, **2008**; b) J. L. Alonso, J. C. López, in *Gas-Phase IR Spectroscopy and Structure of Biological Molecules*, Springer International Publishing, Cham, **2015**, p. 335; c) E. R. Alonso, I. León, J. L. León, *Intra- and Intermolecular Interactions between Non-covalently Bonded Species*, Elsevier, Amsterdam, **2021**, pp. 93–14.

[14] C. Cabezas, I. Peña, J. C. López, J. L. Alonso, *J. Phys. Chem. Lett.* **2013**, *4*, 486–490.

[15] I. León, E. R. Alonso, S. Mata, C. Cabezas, J. L. Alonso, *Angew. Chem. Int. Ed.* **2019**, *58*, 16002–16007; *Angew. Chem.* **2019**, *131*, 16148–16153.

[16] C. Cabezas, M. Varela, J. L. Alonso, *Angew. Chem. Int. Ed.* **2017**, *56*, 6420–6425; *Angew. Chem.* **2017**, *129*, 6520–6525.

[17] C. Cabezas, M. Varela, V. Cortijo, A. I. Jiménez, I. Peña, A. M. Daly, J. C. López, C. Cativiela, J. L. Alonso, *Phys. Chem. Chem. Phys.* **2013**, *15*, 2580.

[18] C. Cabezas, M. A. T. Robben, A. M. Rijs, I. Peña, J. L. Alonso, *Phys. Chem. Chem. Phys.* **2015**, *17*, 20274–20280.

[19] I. León, E. R. Alonso, S. Mata, C. Cabezas, M. A. Rodríguez, J.-U. Grabow, J. L. Alonso, *Phys. Chem. Chem. Phys.* **2017**, *19*, 24985–24990.

[20] a) J. L. Alonso, I. Peña, J. C. López, V. Vaquero, *Angew. Chem. Int. Ed.* **2009**, *48*, 6141–6143; b) I. León, N. Tasinato, L. Spada, et al., *ChemPlusChem* **2021**, *86*, 1374–1386; c) J. L. Alonso, M. A. Lozoya, I. Peña, J. C. López, C. Cabezas, S. Mata, S. Blanco, *Chem. Sci.* **2014**, *5*, 515–522; d) J. L. Alonso, V. Vaquero, I. Peña, J. C. López, S. Mata, W. Caminati, *Angew. Chem. Int. Ed.* **2013**, *52*, 2331–2334; *Angew. Chem.* **2013**, *125*, 2387–2390, and references therein.

[21] S. Ferrer, A. M. Echavarren, *Angew. Chem. Int. Ed.* **2016**, *55*, 11178–11182; *Angew. Chem.* **2016**, *128*, 11344–11348.

[22] a) P. R. McGonigal, C. de León, Y. Wang, A. Homs, C. R. Solorio-Alvarado, A. M. Echavarren, *Angew. Chem. Int. Ed.* **2012**, *51*, 13093–13096; *Angew. Chem.* **2012**, *124*, 13270–13273; b) M. Mato, M. Montesinos-Magraner, A. R. Sugranyes, A. M. Echavarren, *J. Am. Chem. Soc.* **2021**, *143*, 10760–10769.

[23] C. Bermúdez, I. Peña, S. Mata, J. L. Alonso, *Chem. Eur. J.* **2016**, *22*, 16829, and references therein.

[24] H. M. Pickett, *J. Mol. Spectrosc.* **1991**, *148*, 371–377.

[25] Gaussian 16, Revision A.03, M. J. Frisch, G. W. Trucks, H. B. Schlegel, G. E. Scuse-ria, M. A. Robb, J. R. Cheeseman, G. Scalmani, V. Barone, G. A. Peters-son, H. Nakatsuji, X. Li, M. Caricato, A. V. Marenich, J. Bloino, B. G. Janesko, R. Gomperts, B. Mennucci, H. P. Hratchian, J. V. Ortiz, A. F. Izmaylov, J. L. Sonnenberg, D. Williams-Young, F. Ding, F. Lipparini, F. Egidi, J. Goings, B. Peng, A. Petrone, T. Henderson, D. Ranasinghe, V. G. Zakrzewski, J. Gao, N. Rega, G. Zheng, W. Liang, M. Hada, M. Ehara, K. Toyota, R. Fukuda, J. Hasegawa, M. Ishida, T. Nakajima, Y. Honda, O. Kitao, H. Nakai, T. Vreven, K. Throssell, J. A. Montgomer-y Junior, J. E. Peralta, F. Ogliaro, M. J. Bearpark, J. J. Heyd, E. N. Brothers, K. N. Kudin, V. N. Staroverov, T. A. Keith, R. Kobayashi, J. Normand, K. Raghavachari, A. P. Rendell, J. C. Burant, S. S. Iyengar, J. Tomasi, M. Cossi, J. M. Millam, M. Klene, C. Adamo, R. Cammi, J. W. Ochterski, R. L. Martin, K. Morokuma, O. Farkas, J. B. Foresman, D. J. Fox, Gaussian, Inc., Wallingford CT, **2016**.

[26] a) M. Sanz-Novo, E. R. Alonso, I. León, J. L. Alonso, *Chem. Eur. J.* **2019**, *25*, 10748–10755; b) E. R. Alonso, I. León, L. Kolesniková, J. L. Alonso, *ChemPhysChem* **2018**, *19*, 3334–3340; c) S. Oswald, M. A. Suhm, *Phys. Chem. Chem. Phys.* **2019**, *21*, 18799–18810.

[27] a) D. Schmitz, V. A. Shubert, T. Betz, M. Schnell, *J. Mol. Spectrosc.* **2012**, *280*, 77–84 and references therein; b) G. T. Fraser, R. D. Suenram, C. L. Lugez, *J. Phys. Chem. A* **2001**, *105*, 9859–9864, and references therein.

[28] J. Kraitchman, *Am. J. Phys.* **1953**, *21*, 17.

[29] L. Kolesniková, I. León, E. R. Alonso, S. Mata, J. L. Alonso, *Angew. Chem. Int. Ed.* **2021**, *60*, 24461–24466; *Angew. Chem.* **2021**, *133*, 24666–24671.

[30] A. N. Bismillah, B. M. Chapin, B. A. Hussein, P. R. McGonigal, *Chem. Sci.* **2020**, *11*, 324.